J. Hydrol. Hydromech., 70, 2022, 3, 269–275
https://doi.org/10.2478/johh-2022-0016
©2022 Miroslav Fér et al., published by Sciendo. This work is licensed under the Creative Commons Attribution-NonCommercial-NoDerivatives 4.0 International Licence.

sciendo Journal of Hydrology and Hydromechanics Institute of Hydrology SAS

How various mulch materials can affect the soil hydro-physical properties

Miroslav Fér*, Antonín Nikodem, Sára Trejbalová, Aleš Klement, Lenka Pavlů, Radka Kodešová

Czech University of Life Sciences Prague, Kamýcká 129, 16500, Praha Suchdol, Czech Republic.
* Corresponding author. E-mail: mfer@af.czu.cz

Abstract: An application of different mulch materials may lead to changes in soil properties. Our previous study, focused on the impact of various mulches during the 4-year period, showed that the change in some properties can be very rapid (e.g., soil pH), but in other cases such as hydraulic properties, the changes can be gradual. To find out, whether the extension of the mulching period will further affect the studied soil properties, the experiment continued for another 2 years. Differences between values of organic carbon content (C_{ox}), soil physical quality (S_{inf}), gravitational water (GW) and readily available water (RAW) of soils not covered by any mulch and under various mulches (bark chips; wood chips; wheat straw; Agrotex EKO+ decomposable matting; polypropylene fabric covered bark chips; crushed stone) were much larger than those observed in our previous study. On the other hand, the opposite trend was observed for the water stable aggregates (WSA) index or soil pH. Differences between additionally measured hydraulic conductivities at the pressure head of −2 cm and repellency index (RI) were mostly insignificant. Results indicated that organic mulches can either positively (e.g., increase WSA index and C_{ox}, and decrease GW) or negatively (e.g., decrease S_{inf} and RAW, and increase RI) affect soil properties.

Keywords: Mulch; Aggregate stability; Soil hydraulic properties; Soil physical quality; Repellency index; Readily available water.

INTRODUCTION

Mulching is a technology used in agriculture and horticulture to reduce weeds, improve water and thermic soil regimes, and protect soil from erosion (Nzeyimana et al., 2017; Rees et al., 2002). A variety of mulching materials are currently available, such as polyethylene foils, nonwoven fabrics, biodegradable plastic foils, paper films, organic mulches, such as straw or wood chips, and also gravels. The choice of material to cover the soil surface depends on the land use. Some mulch types are used in open or greenhouse agriculture systems. Wood chips or gravels are preferred in gardening. Different materials then have different effects on soil water and thermic regimes, and consequently also on other soil properties (e.g., Al-Shammary et al., 2020; Hlaváčiková et al. 2019; Kader et al., 2017; Kasirajan and Ngouajio, 2012; Kodešová et al., 2014; Pavlů et al., 2021; Qu et al., 2019; Thai et al., 2022; Wang et al., 2021; Yang et al., 2020). For instance, Pavlů et al. (2021) studied soil properties in 27 perennial patches covered by eight different mulch materials (bark chips, wood chips, wheat straw, cardboard, paper foil, decomposable matting, nonwoven fabric covered by bark chips, and crushed basalt) and control patches without any mulch during the 4-year period. The results showed that organic carbon content (C_{ox}), aggregate stability, and pH mostly did not show any trends over time, except for C_{ox} and aggregate stability from patches with bark or wood chips and wheat straw. In these cases, decomposed organic matter significantly increased both properties. On the other hand, the soil hydraulic properties (mostly due to no-till practice) considerably changed in all patches. The saturated and residual water contents, saturated hydraulic conductivity, and reciprocal of the air-entry pressure head increased. Correspondingly, the bulk density decreased. Soil water retention curves from the patches with bark or wood chips were more gradual than those from other patches, which indicates higher water retention capacity for lower pressure heads. However, the physical quality of soils under organic mulches expressed by the slope at the retention curve inflection point was lower than that for other scenarios. Readily available water under organic mulches was also lower than that for other setups. Study also showed that the one-year effect on soil hydraulic properties was negligible in comparison to much greater impact after 4 years. Therefore, this study was extended with the objective to evaluate, if the mulches, which were not decomposed or could be refilled, can affect soil properties even more after another two-year period.

MATERIALS AND METHODS

The experiment was carried out on the field of the experimental station of the Czech University of Life Sciences Prague in Prague-Troja (Czech Republic). According to the Köppen-Geiger climate classification (Kottek et al., 2006), the region can be classified as Cfb climate; a warm temperated humid climate, all months with average temperatures below 22 °C and four or more months with average temperatures above 10 °C. The soil type in this area is a Haplic Fluvisol (IUSS, 2014; Zádorová et al., 2020) developed on fluvial sediments of the Vltava River. Formerly, the field was commonly cultivated and used for crop production. The multidisciplinary study combining soil science and gardening (perennials surviving) was set up in April 2015. Details about the experimental setup and results obtained during the four-year period (2015–2018) have been discussed by Pavlů et al. (2021). The experiment continued for another 2 years. At the end, in July 2020, patches (three replicates for each scenario) with sufficient coverage of mulching materials were examined: NMU–Not mulched control patch; ATE–Agrotex EKO+ decomposable matting; NFB–Polypropylene nonwoven fabric covered bark chips layer; BRK–Bark chips; WCH–Wood chips; STR–Wheat straw; CRS–Crushed stone.

In every patch the mulch material has been carefully removed. The particle size distribution was evaluated before by Pavlů et al. (2021): 14% of clay, 23% of silt and 63% of sand. The other chemical and physical properties were measured in three replicates on the grab soil samples using the standardized laboratory techniques: active and exchangeable pH values (pH_{H2O} and pH_{CaCl2}, respectively) (ISO 10390, 2005), soil salinity in water (Rhoades, 1996), oxidable organic carbon content (C_{ox}) (Skjemstad and Baldock, 2008), aggregate stability assessed using the WSA index (Nimmo and Perkins, 2002). In addition, no content of $CaCO_3$ (Loeppert and Suarez, 1996) was found in all cases.

Soil water retention curves (SWRC) were obtained on the 100-cm^3 undisturbed soil samples (6 replicates for each mulching scenario) using the pressure plate apparatus (Dane and Hopmans, 2002). Initially fully saturated soil samples (using the saturation pan) placed into the pressure plate extractors (Soilmoisture Equipment Corp., 2009) were drained in 8 pressure head steps (−1, −40, −100, −700, −2000, −5000, −8000, and −15000 cm). Equilibrium water contents (θ) at each executed pressure head step (h), were determined gravimetrically. The RETC Program (van Genuchten et al., 1991) was applied to fit the experimental SWRC data points ($\theta(h)$) using the van Genuchten (1980) equation:

$$\theta_e = \frac{\theta - \theta_r}{\theta_s - \theta_r} \quad \theta_e = \frac{1}{(1 + (\alpha|h|)^n)^m}, \quad h < 0 \quad \theta_e = 1, \quad h \geq 0 \tag{1}$$

where θ_e is the effective soil water content (dimensionless), θ_r is the residual soil water content [L^3/L^3], θ_s is the saturated water content [L^3/L^3], α is the reciprocal of the air-entry pressure head [1/L], and n (dimensionless) is related to the slope of the retention curve at the inflection point (dimensionless).

The parameters of the inflection points, i.e., soil water content (θ_{inf}), the pressure head (h_{inf}) and curve slope (S_{inf}), of the soil water retention curves were also computed according to Dexter (2004a, b, c) and Dexter and Czyz (2007):

$$h_{inf} = \frac{1}{\alpha}\left(\frac{1}{m}\right)^{\frac{1}{n}} \tag{2}$$

$$\theta_{inf} = (\theta_s - \theta_r)\left(1 + \frac{1}{m}\right)^{-m} + \theta_r \tag{3}$$

$$S_{inf} = -n(\theta_s - \theta_r)\left(1 + \frac{1}{m}\right)^{-(1+m)} \tag{4}$$

These parameters can be used to assess a physical quality of soils (e.g., Dexter, 2004a, b, c; Fér et al., 2016, 2018, 2020; Jirků et al., 2013; Pavlů et al., 2021): if $S_{inf} \geq 0.05$, the physical quality of soil (PQS) is very good; if $0.05 > S_{inf} \geq 0.035$, PQS is good; if $0.035 > S_{inf} \geq 0.02$, PQS is poor; and if $0.02 > S_{inf}$, PQS is very poor. The bulk density (ρ_d) and total porosity (P) were determined on the undisturbed soil samples after measurements of the soil water retention curves by Dane and Topp (2002).

In addition, the amounts of gravitational water (GW) and readily available water (RAW) were expressed in mm of water per 1 cm soil layer as follows:

$$\mathrm{GW} = 10(\theta_s - \theta_{100}) \tag{5}$$

$$\mathrm{RAW} = 10(\theta_{100} - \theta_{250}) \tag{6}$$

where θ_{100} and θ_{250} are the soil water contents for the pressure heads of −100 and −250 cm, respectively.

The mini disk tension infiltrometer with a disk radius of 2.22 cm by Meter Group Inc. (Munich, Germany) was used to assess the unsaturated hydraulic conductivity and sorptivity. Cumulative infiltrations of water or ethanol were measured in four replicates at each patch. Pressure head was always set at the value of −2 cm according to Watson and Luxmoore (1986) as limit between gravitational and capillary pores. The close contact between the carefully levelled soil surface and disk was ensured by a 1 mm layer of the same soil, sieved through a 2-mm sieve, as proposed by Kodešová et al. (2010, 2011). The infiltration test lasted at least 30 min. The method proposed by Zhang et al. (1997) was used to evaluate the unsaturated hydraulic conductivity for pressure head of −2 cm ($K_{h\,=\,-2\ cm,\ Z}$). Cumulative water infiltration (I) [L] in time (t) [T] was fitted using the following equation:

$$I = C_1 t + C_2 t^{1/2} \tag{7}$$

C_1 [L/T] and C_2 [L/T] are parameters related to the hydraulic conductivity $K(h_0)$ and sorptivity $S(h_0)$:

$$C_1(h_0) = A_1 K(h_0) \quad \text{and} \quad C_2(h_0) = A_2 S(h_0) \tag{8}$$

where A_1 [L/T] and A_2 [L/T] are dimensionless constants. The $K(h_0)$ value was calculated using Eq. (5) and the following expressions for the A_1 constant:

$$A_1 = \frac{11.65(n^{0.1} - 1)\exp[2.92(n - 1.9)ah_0]}{(ar_0)^{0.91}} \quad \text{for } n \geq 1.9 \tag{9}$$

$$A_1 = \frac{11.65(n^{0.1} - 1)\exp[7.5(n - 1.9)ah_0]}{(ar_0)^{0.91}} \tag{10}$$

for $1.35 \leq n < 1.9$

$$A_1 = \frac{11.65(n^{0.82} - 1)\exp[34.65(n - 1.19)\alpha h_0]}{(\alpha r_0)^{0.6}} \tag{11}$$

for $n < 1.35$

where α and n are the van Genuchten parameters (parameters obtained from the pressure plate experiment), r_0 is the disk radius (2.22 cm) and h_0 is the applied pressure head (−2 cm).

Another method proposed by Wooding (1968) was also used to evaluate the unsaturated hydraulic conductivity ($K_{h\,=\,-2\ cm,\ W}$) from the disk infiltrometer measurements. The following algebraic approximation of steady state unconfined infiltration rates into soil from a circular source of radius r_0 [L] was assumed:

$$Q = \pi r_0^2 K(h_0)\left(1 + \frac{4}{\pi r_0 \alpha_G}\right) \tag{12}$$

where Q is the steady water flux [L^3/T], and α_G [1/L] is the constant in Gardner equation (1958) describing the relationship between the unsaturated hydraulic conductivity and the pressure head.

$$K(h) = K_s \exp(\alpha_G h) \tag{13}$$

value α_G characterizing soil structure was measured by Reynolds and Elrick (1991) as follows: for sand, 0.36 1/cm, loam, 0.12 1/cm and clay, 0.04 1/cm. The value for loam was applied in this study to evaluate the $K(h_0)$ values.

The sorptivities (S) for both liquids (water sorptivity, S_w, and ethanol sorptivity, S_e) were estimated from their cumulative infiltrations, (I), during the early-time infiltration process (Philip, 1957):

$$S(-2\ \text{cm}) = I/t^{1/2} \quad (14)$$

The repellency index (RI) was calculated:

$$\text{RI} = 1.95\ S_e/S_w \quad (15)$$

All 16 combinations of four S_e values and four S_w values for each spot were examined as proposed by Pekárová et al. (2015). The resulting RI values were judged according to the new classification published by Iovino et al. (2018): when RI < 1.95, soil is wettable; when 1.95 ≤ RI < 10, soil is slightly water repellent; when 10 ≤ RI < 50, soil is strongly water repellent; when 50 ≤ RI < 110, soil is severely water repellent; and when 110 ≤ RI, soil is extremely water repellent.

Statistical analyses were performed using STAGRAPHICS Centurion XV Version 15.2.06. First, the normality of all data sets was tested (Kolmogorov-Smirnov and Liliefors test). Outliers (based on the three-sigma rule of thumb (Upton and Cook, 2008)) of each variable were excluded from the dataset. The multiple range tests were used to compare the values of a particular soil property resulting from different scenarios. Simple correlations between measured chemical, physical and hydraulic soil properties were assessed using the Pearson product moment correlation coefficient. The statistical significance was tested using the p-value.

RESULTS AND DISCUSSION

The resulting soil properties and parameters are shown in Table 1 and Figure 1. The similar C_{ox} contents (Table 1) were found in the soils under foils ATE and NFB, crushed stone (CRS), mulched control plots (NMU) and wheat straw (STR). The C_{ox} contents in the soils under organic materials such as bark (BRK) and wood chips (WCH) and were significantly larger. The highest value of C_{ox} content was measured for soils under the bark chips mulch. The soil structure stability evaluated using the WSA index (Table 1) was lowest at the control patch without mulch. The high WSA index was again determined for the scenario under bark chips. Differences between the C_{ox} values measured under organic mulches and other cover were much larger than those observed in 2018 (Pavlů et al., 2021). On the other hand, the opposite trend (i.e., smaller differences between values for different scenarios) was observed for the WSA values. Interestingly, differences between both pH values (i.e., pH_{H2O} and pH_{CaCl2}, Table 1) for different scenarios were also much smaller (or even statistically insignificant) in comparison to that observed by Pavlů et al. (2021). This indicates that the immediate impact of various mulches on soil pH, which resulted in high differences between the values from different scenarios (Pavlů et al., 2021), diminished. The reason in both cases can be a gradual decomposition of all mulches and leaching of the selected compounds towards groundwater that resulted in different composition of aggregate's cementing agents in time (Thai et al., 2022). The EC values in Table 1 (which were not measured in our previous study) showed that the salinity under organic mulches (particularly under WCH cover) was much larger than that for the control plots (NMU) and the CRS plots. This associated with an extensive decomposition of the applied organic materials and their compositions (Bang-Andreasen et al., 2017; Dissanayake et al., 2022; Qu et al., 2019), and corresponds with the larger differences between the Cox values resulted from various scenarios (i.e., a positive correlation between C_{ox} and EC, Table 2).

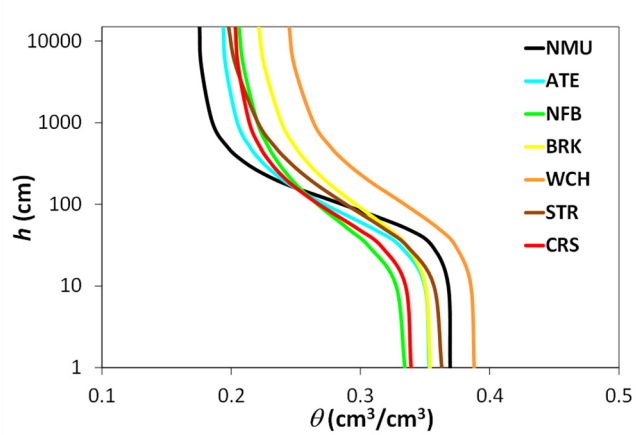


Fig. 1. Mean soil water retention curves (SWRC) of the soils under various mulches: NMU—Not mulched control patch, ATE—Agrotex EKO+ decomposable matting, NFB—Polypropylene nonwoven fabric covered with bark chips layer, BRK—Bark chips, WCH—Wood chips, STR—Wheat straw, and CRS—Crushed stone.

SWRC from the not mulched control plots (NMU) differed from those of other mulched soils (Figure 1), which was also proved by the significant difference between the *n* values for NMU and those for other scenarios (Table 1). It seems that the shapes of the SWRC under different mulching materials did not considerably vary (Figure 1) and SWRC differed mainly in their θ_s values (Table 1). However, statistical analyses of the van Genuchten hydraulic parameters (Table 1) revealed statistically significant differences between all van Genuchten hydraulic parameters for different scenarios. A very similar shape but θ_s shift was observed for SWRC for bark chips (BRK) and wood chips (WCH). The same shapes of these curves were also observed by Pavlů et al. (2021). Interestingly, entire SWRC for soil under crushed stone (CRS) was similar to that under foil NFB. It should be noted that all curves differed from those presented by Pavlů et al. (2021) likely also due to a different method for SWRC measurement (i.e., multi-step outflow test) used in our previous study. The reason is that the pressure plate extractor method cannot sufficiently measure soil water contents close to saturation. Which is documented here by large differences between the θ_s and *P* values (Table 1). The porosity was highest for wood chips scenario (WCH), followed by bark chips (BRK) and not mulched control plots (NMU).

The physical quality of soil evaluated based on the inflection points of SWRC (Table 1) was very good for control plots without mulch (NMU) and soils under ATE (i.e., $S_{inf} > 0.05$ (Dexter, 2004a, b, c; Dexter and Czyz, 2007). These S_{inf} values were significantly larger than values for other scenarios, which varied between 0.05 and 0.035 and indicated a good physical quality. The larger S_{inf} values for NMU and ATE in comparison to the S_{inf} values for other scenarios were also observed in our previous study (Pavlů et al., 2021), but differences between scenarios were not statistically significant. This may imply a pronounced temporal trend in the impact of different covers on soil physical quality. Similarly, statistical analyses of the GW and RAW values (i.e., homogeneous groups in Table 1) show greater diversity between different scenarios in comparison to that observed by Pavlů et al. (2021). For instance, the GW values for NMU and ATE are significantly larger that the GW values for BRK and WCH (i.e., scenarios with large sources of organic matter from these two mulch materials) or the RAW values for NMU were significantly larger that the RAW values for all other scenarios. Such statistically significant differences were not observed before (Pavlů et al., 2021).

Table 1. Mean values (per each mulch variant) and standard deviations of pH in H_2O or $CaCl_2$ soil extract, salinity (EC), water stable aggregate index (WSA), organic carbon content (C_{ox}), porosity (P), bulk density (ρ_d), field soil water content (θ_{field}), hydraulic conductivity for h = –2 cm evaluated using the Wooding method ($K_{h=-2cm, W}$) and the Zhang method ($K_{h=-2 cm, Z}$), repellency index (RI), saturated soil water content (θ_s), residual soil water content (θ_r), parameters α and n, retention curve slope at the inflection point (S_{inf}), absolute value of the negative pressure head at the inflection point (h_{inf}), soil water content at the inflection point (θ_{inf}), gravitational water (GW), and readily available water (RAW). Letters a, b, c, d and e represent homogeneous groups (HG). NMU–Not mulched control patch, ATE–Agrotex EKO+ decomposable matting, NFB–Polypropylene nonwoven fabric covered with bark chips layer, BRK–Bark chips, WCH–Wood chips, STR–Wheat straw, CRS–Crushed stone.

	pH_{H2O} (–)			pH_{CaCl2} (–)			EC (µS/cm)			WSA (–)		
	Mean	St.Dev.	HG	Mean	St.Dev.	HG	Mean	St.Dev.	HG	Mean	St.Dev.	HG
NMU	6.98	0.04	c	6.12	0.05	a	77.2	5.9	a,b	0.765	0.066	a
ATE	6.89	0.05	b,c	6.15	0.02	a	100.5	15.2	a,b,c	0.772	0.025	a,b
NFB	6.71	0.07	a,b	5.96	0.08	a	93.4	21.1	a,b,c	0.788	0.029	a
BRK	6.59	0.23	a	6.03	0.25	a	114.9	24.1	b,c	0.792	0.052	a,b
WCH	6.85	0.02	b,c	6.03	0.10	a	129.6	17.7	c	0.836	0.037	b
STR	6.87	0.04	b,c	6.07	0.04	a	102.2	22.9	a,b,c	0.784	0.032	a,b
CRS	6.91	0.19	b,c	6.13	0.03	a	74.5	16.5	a	0.801	0.063	a,b
	C_{OX} (%)			P (cm^3/cm^3)			ρ_d (g/cm^3)			θ_{field} (cm^3/cm^3)		
	Mean	St.Dev.	HG	Mean	St.Dev.	HG	Mean	St.Dev.	HG	Mean	St.Dev.	HG
NMU	1.83	0.16	a	0.465	0.022	b,c	1.42	0.06	b,c	0.150	0.017	a
ATE	2.02	0.17	a	0.453	0.019	a,b	1.45	0.05	a,b	0.167	0.095	a
NFB	1.98	0.20	a	0.454	0.011	a,b	1.45	0.03	a,b	0.251	0.029	a,b
BRK	3.36	0.31	b	0.471	0.035	b,c	1.40	0.09	b,c	0.232	0.082	a,b
WCH	3.00	0.10	b	0.485	0.014	c	1.37	0.04	c	0.294	0.017	b
STR	2.34	0.36	a	0.448	0.026	a,b	1.46	0.07	a,b	0.159	0.085	a
CRS	1.85	0.29	a	0.440	0.012	a	1.48	0.03	a	0.251	0.031	a,b
	$K_{h=-2 cm, W}$ (cm/h)			$K_{h=-2 cm, Z}$ (cm/h)			RI (–)			θ_S (cm^3/cm^3)		
	Mean	St.Dev.	HG	Mean	St.Dev.	HG	Mean	St.Dev.	HG	Mean	St.Dev.	HG
NMU	0.25	0.154	a,b	0.073	0.045	a	3.5	4.6	a	0.369	0.016	c,d
ATE	0.18	0.072	a	0.064	0.037	a	5.3	6.3	a	0.353	0.004	a,b,c
NFB	0.41	0.260	b	0.118	0.219	b	2.0	2.5	a	0.335	0.016	a
BRK	0.23	0.078	a,b	0.041	0.046	a	21.7	12.3	a	0.354	0.028	a,b,c
WCH	0.24	0.156	a,b	0.281	0.314	a	4.0	6.3	a	0.388	0.021	d
STR	0.29	0.194	a,b	0.021	0.015	b	2.5	2.1	a	0.363	0.019	b,c,d
CRS	0.30	0.192	a,b	0.312	0.189	a	9.0	13.9	a	0.339	0.005	a,b
	θ_r (cm^3/cm^3)			α (1/cm)			n (–)			S_{inf}		
	Mean	St.Dev.	HG	Mean	St.Dev.	HG	Mean	St.Dev.	HG	Mean	St.Dev.	HG
NMU	0.175	0.013	a	0.013	0.001	a	2.17	0.22	c	0.084	0.012	c
ATE	0.193	0.018	a,b,c	0.020	0.002	b	1.88	0.11	b	0.056	0.008	b
NFB	0.201	0.016	b,c	0.032	0.004	d	1.59	0.14	a	0.035	0.006	a
BRK	0.215	0.017	c	0.020	0.003	b	1.63	0.18	a	0.039	0.010	a
WCH	0.241	0.016	d	0.016	0.003	a	1.70	0.06	a,b	0.044	0.004	a
STR	0.191	0.019	a,b	0.024	0.004	c	1.58	0.12	a	0.044	0.003	a
CRS	0.201	0.013	b,c	0.024	0.005	c	1.79	0.16	a,b	0.045	0.011	a
	h_{inf} (cm)			θ_{inf} (cm^3/cm^3)			GW (mm/cm)			RAW (mm/cm)		
	Mean	St.Dev.	HG	Mean	St.Dev.	HG	Mean	St.Dev.	HG	Mean	St.Dev.	HG
NMU	100	8	c,d	0.286	0.007	a	0.83	0.09	d	0.64	0.10	e
ATE	77	8	a,b	0.287	0.009	a	0.81	0.10	d,e	0.40	0.06	d
NFB	61	2	a	0.284	0.018	a	0.68	0.08	b,c	0.25	0.03	a
BRK	98	24	c,d	0.300	0.022	a	0.57	0.15	a,b	0.31	0.06	a,b
WCH	113	28	d	0.330	0.018	b	0.54	0.07	a	0.37	0.04	c,d
STR	83	15	b,c	0.298	0.018	a	0.74	0.08	c,d,e	0.35	0.03	b,c,d
CRS	71	13	a,b	0.283	0.007	a	0.71	0.10	c,d	0.31	0.07	b,c

The soil properties assessed using the mini disk tension infiltrometer were not investigated in our previous study. The values of $K_{h=-2 cm}$ strongly depended on a method of evaluation (Nikodem et al., 2021). The largest values of the soil hydraulic conductivity ($K_{h=-2 cm, W}$) were obtained for the NFB plot and the lowest values for the ATE plot. In the case of the other method, the largest value of soil hydraulic conductivity ($K_{h=-2 cm, Z}$) was obtained for the WCH plot and the lowest for the STR plot. However, due to a large variability of measured values, differences between various scenarios were mostly statistically insignificant. Similarly, no significant differences were observed between the RI values due to their very large variability. Nevertheless, the highest value of RI was obtained for the BRK plot and the lowest for the NFB scenario.

Table 2, which shows correlation between all evaluated soil parameters, proved relationships observed in our previous study, e.g. positive correlation between and θ_{inf} and WSA or C_{ox}, and negative correlations between GW and WSA or C_{ox}. This again indicate that organic mulches have largest impacts on soil conditions, which can be either favorable (e.g., larger C_{ox} content and WSA) or adverse (e.g., lower S_{inf} and RAW). Interestingly the correlation analyses did not show any relationship between the RI values and parameters that should affect soil water repellency (e.g., C_{ox} content or soil pH) (Sándor et al., 2021; Šurda et al., 2021; Toková et al., 2022).

Table 2. Correlation coefficients of the relationships among the studied soil properties: pH in H_2O or $CaCl_2$ soil extract, salinity (EC), water stable aggregate index (WSA), organic carbon content (C_{OX}), porosity, (P), bulk density (ρ_d), field soil water content (θ_{field}), hydraulic conductivity for $h = -2$ cm evaluated using the Wooding method ($K_{h=-2\ cm,\ W}$) and the Zhang method ($K_{h=-2\ cm,\ Z}$), repellency index (RI), saturated soil water content (θ_s), residual soil water content (θ_r), parameters α and n, retention curve slope at the inflection point (S_{inf}), absolute value of the negative pressure head at the inflection point (h_{inf}), soil water content at the inflection point (θ_{inf}), gravitational water (GW), and readily available water (RAW).

	pH_{H2O}	pH_{CaCl2}	EC	WSA	C_{OX}	P	ρ_d	θ_{field}	$K_{h=-2\ cm,\ W}$	$K_{h=-2\ cm,\ Z}$
pH_{H2O}	1									
pH_{CaCl2}	0.719	1								
EC	–0.481	–0.461	1							
WSA	–0.189	–0.394	0.616	1						
C_{ox}	–0.663	–0.435	0.855*	0.550	1					
P	–0.260	–0.367	0.727	0.491	0.710	1				
ρ_d	0.252	0.364	–0.725	–0.488	–0.703	–0.999***	1			
θ_{field}	–0.417	–0.553	0.421	0.877**	0.427	0.373	–0.369	1		
$K_{h=-2\ cm,\ W}$	–0.223	–0.638	–0.315	0.057	–0.327	–0.350	0.351	0.306	1	
$K_{h=-2\ cm,\ Z}$	0.249	0.034	–0.028	0.736	–0.059	0.066	–0.065	0.747	0.149	1
RI	–0.655	–0.038	0.219	0.071	0.636	0.196	–0.187	0.198	–0.331	–0.109
θ_s	0.310	0.082	0.561	0.389	0.441	0.747	–0.750	–0.002	–0.536	0.067
θ_r	–0.443	–0.486	0.796*	0.934**	0.742	0.628	–0.624	0.865*	–0.071	0.537
α	–0.413	–0.506	–0.184	–0.053	–0.255	–0.588	0.591	0.209	0.799*	–0.037
n	0.674	0.673	–0.524	–0.471	–0.481	0.051	–0.057	–0.484	–0.419	–0.017
S_{inf}	0.693	0.625	–0.465	–0.541	–0.440	0.078	–0.084	–0.637	–0.411	–0.200
h_{inf}	0.069	0.041	0.551	0.378	0.628	0.853*	–0.853*	0.091	–0.560	0.053
θ_{inf}	–0.148	–0.323	0.867*	0.806*	0.756*	0.794*	–0.792*	0.512	–0.303	0.301
GW	0.660	0.662	–0.748	–0.846*	–0.832*	–0.609	0.602	–0.844*	–0.088	–0.383
RAW	0.666	0.555	–0.331	–0.450	–0.311	0.209	–0.216	–0.607	–0.446	–0.215
	RI	θ_S	θ_r	α	n	S_{inf}	h_{inf}	θ_{inf}	GW	RAW
RI	1									
θ_s	–0.166	1								
θ_r	0.273	0.361	1							
α	–0.138	–0.784*	–0.063	1						
n	–0.180	0.235	–0.536	–0.669	1					
S_{inf}	–0.262	0.354	–0.613	–0.689	0.959***	1				
h_{inf}	0.216	0.909**	0.420	–0.860*	0.268	0.3401	1			
θ_{inf}	0.061	0.797*	0.832*	–0.417	–0.310	–0.2562	0.760*	1		
GW	–0.444	–0.239	–0.936**	–0.053	0.640	0.6843	–0.384	–0.745	1	
RAW	–0.259	0.503	–0.519	–0.763*	0.910**	0.983***	0.482	–0.099	0.584	1

*** p<0.001, ** p<0.01, * p<0.05

CONCLUSIONS

Study focused on the evaluation if the extended time of soil cover by various mulches increases the differences between the measured soil properties. Prolonged period of soil exposure to various soil and thermal regimes mostly increased differences between the evaluated parameters (e.g., C_{ox}, S_{inf}, GW and RAW). On the other hand, the impact of different covers on soil pH, which was very quick at the beginning of the experiment (Pavlů et al., 2021), diminished during the extended period. Interestingly, also the WSA index displayed smaller variability despite that other parameter that affects soil aggregate stability were more diverse. This extended study again proved that organic mulches can either improve (e.g., increase C_{ox} content and aggregate stability) or aggravate (e.g., decrease soil physical quality and amount of readily available water, and increase water repellency) soil properties.

Acknowledgements. The authors acknowledge the financial support of the European Structural and Investment Funds, projects NutRisk (No. CZ.02.1.01/0.0/0.0/16_019/0000845).

REFERENCES

Al-Shammary, A.A.G., Kouzani, A., Gyasi-Agyei, Y., Gates, W., Rodrigo-Comino, J., 2020. Effects of solarisation on soil thermal-physical properties under different soil treatments: a review. Geoderma, 363, 114137.

Bang-Andreasen, T., Nielsen, J.T., Voriskova, J., Heise, J., Rønn, R., Kjøller, R., Hansen, H.C.B., Jacobsen, C.S., 2017. Wood ash induced pH changes strongly affect soil bacterial numbers and community composition. Front. Microbiol., 8, 1400.

Dane, J.H., Hopmans, J.W., 2002. Water retention and storage. In: Dane, J.H., Topp, G.C. (Eds.): Methods of Soil Analysis. Part 4. Physical Methods. SSSA Book Series No. 5. Soil Science Society of America Madison USA. ISBN: 0–89118–841–X.

Dane, J.H., Topp, G.C., 2002. Methods of Soil Analysis. Part 4. Physical Methods. SSSA, Madison, WI, 1692 p.

Dexter, A.R, Czyz, E.A., 2007. Application of S–theory in study of soil physical degradation and its consequences. Land Degrad. Dev., 18, 369–381.

Dexter, A.R., 2004a. Soil physical quality Part I. Theory effect of soil texture density and organic matter and effect on root growth. Geoderma, 120, 201–214.

Dexter, A.R., 2004b. Soil physical quality Part II. Friability tillage tilth and hard–setting. Geoderma, 120, 215–226.

Dexter, A.R., 2004c. Soil physical quality Part III. Unsaturated hydraulic conductivity and general conclusions about S–theory. Geoderma, 120, 227–239.

Dissanayake, P.D., Palansooriya, K.N., Sang, M.K., Oh, D.X., Park, J., Hwang, S.Y., Igalavithana, A.D., Gu, C., Ok, Y.S., 2022. Combined effect of biochar and soil moisture on soil chemical properties and microbial community composition in microplastic-contaminated agricultural soil. Soil Use Manag., 38, 1–13. https://doi.org/10.1111/sum.12804.

Gardner, W.R., 1958. Some steady state solutions of unsaturated moisture flow equations with application to evaporation from a water table. Soil Sci., 85, 228–232.

Fér, M., Kodešová, R., Hroníková, S., Nikodem, A., 2020. The effect of 12-year ecological farming on the soil hydraulic properties and repellency index. Biologia, 75, 795–798.

Fér, M., Kodešová, R., Nikodem, A., Jelenová, K., Klement, A., 2018. Influence of soil–water content on CO_2 efflux within the elevation transect heavily impacted by erosion. Ecohydrology, 11, 6, e1989.

Fér, M., Kodešová, R., Nikodem, A., Jirků, V., Jakšík, O., Němeček, K., 2016. The impact of the permanent grass cover or conventional tillage on hydraulic properties of Haplic Cambisol developed on paragneiss substrate. Biologia, 71, 10, 1144–1150.

Hlaváčiková, H., Novák, V., Kameyama, K., Brezianská, K., Rodný, M., Vitková, J., 2019. Two types of biochars: one made from sugarcane bagasse, other one produced from paper fiber sludge and grain husks and their effects on water retention. Soil Water Res., 14, 2, 67–75.

Iovino, M., Pekárová, P., Hallett, D.P., Pekár, J., Lichner, Ľ., Mataix-Solera, J., Alagna, V., Walsh, R., Raffan, A., Schacht, K., Rodný, M., 2018. Extent and persistence of soil water repellency induced by pines in different geographic regions. J. Hydrol. Hydromech., 66, 4, 360–368.

ISO 10390, 2005. International Organization of Standardization, 2005. Soil Quality - Determination of pH.

IUSS, 2014. World Reference Base for Soil Resources 2014. World Soil Resources Reports No. 106. FAO, Rome.

Jirků, V., Kodešová, R., Nikodem, A., Mühlhanselová, M., Žigová, A., 2013. Temporal variability of structure and hydraulic properties of topsoil of three soil types. Geoderma, 204–205, 43–58.

Kader, M.A., Senge, M., Mojid, M.A., Nakamura, K., 2017. Mulching type-induced soil moisture and temperature regimes and water use efficiency of soybean under rain-fed condition in central Japan. Int. Soil Water Conserv. Res., 5, 302–308.

Kasirajan, S., Ngouajio, M., 2012. Polyethylene and biodegradable mulches for agricultural applications: a review. Agron. Sustain. Dev., 32, 501–529.

Kodešová, R., Fér, M., Klement, A., Nikodem, A., Teplá, D., Neuberger, P., Bureš, P., 2014. Impact of various surface covers on water and thermal regime of Technosol. J. Hydrol., 519, 2272–2288.

Kodešová, R., Šimůnek, J., Nikodem, A., Jirků, V., 2010. Estimation of parameters of the radially-symmetric dual-permeability model using tension disc infiltrometer and Guelph permeameter experiments. Vadose Zone J., 9, 213–225.

Kodešová, R., Jirků, V., Kodeš, V., Mühlhanselová, M., Nikodem, A., Žigová, A., 2011. Soil structure and soil hydraulic properties of Haplic Luvisol used as arable land and grassland. Soil Till. Res., 111, 2, 154–161.

Kottek, M., Grieser, J., Beck, C., Rudolf, B., Rubel, F., 2006. World map of the Köppen-Geiger climate classification updated. Meteorologische Zeitschrift, 15, 259–263.

Loeppert, R., Suarez, D., 1996. Carbonate and Gypsum. Methods Soil Anal. Part 3-Chemical Methods. In: SSSA B, Ser. No. 5, pp. 437e475.

Meter Group AG, 2020. Mini Disk Infiltrometer. Mettlacher Straße 8, München.

Nikodem, A., Kodešová, R., Fér, M., Klement, A., 2021. Variability of topsoil hydraulic conductivity along the hillslope transects delineated in four areas strongly affected by soil erosion. J. Hydrol. Hydromech., 69, 2, 220–231.

Nimmo, J.R., Perkins, K.S., 2002. Aggregate stability and size distribution. In: Dane, J.H., Topp, G.C. (Eds.): Methods of Soil Analysis, Part 4. Physical Methods. SSSA, Madison, WI, pp. 317–328.

Nzeyimana, I., Hartemink, A.E, Ritsema, C., Stroosnijder, L., Lwanga, E.H., Geissen, V., 2017. Mulching as a strategy to improve soil properties and reduce soil erodibility in coffee farming systems of Rwanda. Catena, 149, 43–51.

Pavlů, L., Kodešová, R., Fér, M., Nikodem, A., Němec, F., Prokeš, R., 2021. The impact of various mulch types on soil properties controlling water regime of the Haplic Fluvisol. Soil Till. Res., 205, 104748.

Pekárová, P., Pekár, J., Lichner, Ľ., 2015. A new method for estimating soil water repellency index. Biologia, 70, 1450–1455.

Philip, J.R., 1957. The theory of infiltration: 1. The infiltration equation and its solution. Soil Sci 83, 345–358.

Qu, B., Liu, Y., Sun, X., Li, S., Wang, X., Xiong, K., Yun, B., Zhang, H., 2019. Effect of various mulches on soil physico–chemical properties and tree growth (*Sophora japonica*) in urban tree pits. PLoS ONE, 14, 2, e0210777.

Rees, H.W., Chow, T.L., Loro, P.J., Lavoie, J., Monteith, J.O., Blaauw, A., 2002. Hay mulching to reduce runoff and soil loss under intensive potato production in northwestern New Brunswick, Canada. Can. J. Soil Sci., 82, 2, 249–258.

Reynolds, W.D., Elrick, D.E., 1991. Determination of hydraulic conductivity using a tension infiltrometer. Soil Sci. Soc. Am. J., 55, 633–639.

Rhoades, J.D., 1996. Salinity: electrical conductivity and total dissolved aolids. In: Sparks, D.L., Page, A.L., Helmke, P.A., Loepert, R.H., Soltanpour, P.N., Tabatabai, M.A. (Eds.), Methods of Soil Analysis. Part 3. Chemical Methods. SSSA, Madison, WI, pp. 417–435.

Sándor, R., Iovino, M., Lichner, L., Alagna, V., Forster, D., Fraser, M., Kollár, J., Šurda, P., Nagy, V., Szabó, A., Fodor, N., 2021. Impact of climate, soil properties and grassland cover on soil water repellency. Geoderma, 383, 114780.

Skjemstad, J., Baldock, J.A., 2008. Total and organic carbon. In: Carter, M. (Ed.): Soil Sampling and Methods of Analysis, 2nd ed. CRC Press, Boca Raton, FL, USA, pp. 225–238.

Soilmoisture Equipment Corp., 2009. 15 Bar pressure plate extractor operating instructions. Soilmoisture Equipment Corp., Santa Barbara, CA.

Šurda, P., Lichner, Ľ., Kollár, J., Zvala, A., Igaz, D., 2021. Evaluation of soil properties in variously aged Scots pine plantations established on sandy soil. J. Hydrol. Hydromech., 69, 3, 347–355.

Thai, S., Davídek, T., Pavlů, L., 2022. Causes clarification of the soil aggregates stability on mulched soil. Soil Water Res., 17, 2, 91–99.

Toková, L., Hološ, S., Šurda, P., Kollár, J., Lichner, Ľ., 2022. Impact of duration of land abandonment on infiltration and surface runoff in acidic sandy soil. Agriculture, 12, 168.

van Genuchten, M.Th., 1980. A closed-form equation for predicting the hydraulic conductivity of unsaturated soils. Soil Sci. Soc. Am. J., 44, 5, 892–898.

Upton, G., Cook, I., 2008. A Dictionary of Statistics, 2nd ed. rev. Oxford University Press, Oxford.

van Genuchten, M.Th., Leij, F.J., Yates, S.R., 1991. The RETC code for quantifying the hydraulic functions of unsaturated soils. EPA report 600/2–91/065. U.S. Salinity Laboratory, USDA-ARS.

Wang, Q., Liu, X., Li, J., Yang, X., Guo, Z., 2021. Straw application and soil organic carbon change: A meta-analysis. Soil

Water Res., 16, 2, 112–120.
Watson, K.W., Luxmoore, R.J., 1986. Estimating macroporosity in a forest watershed by use of a tension infiltrometer. Soil Sci. Soc. Am. J., 50, 578–582.
Wooding, R.A., 1968. Steady infiltration from a shallow circular pond. Water Resour. Res., 4, 1259–1273.
Yang, Y., Li, P., Jiao, J., Yang, Z., Lv, M., Li, Y., Zhou, Ch., Wang, Ch., He, Z., Liu, Y., Song, S., 2020. Renewable sourced biodegradable mulches and their environment impact. Sci. Hortic., 268, 109375.
Zádorová, T., Žížala, D., Penížek, V., Vaněk, A., 2020. Harmonisation of a large-scale historical database with the actual Czech soil classification system. Soil Water Res., 15, 2, 101–115.
Zhang, R., 1997. Determination of soil sorptivity and hydraulic conductivity from the disk infiltrometer. Soil Sci. Soc. Am. J., 61, 1024–1030.

Received 6 June 2022
Accepted 22 June 2022